Graphical Abstract

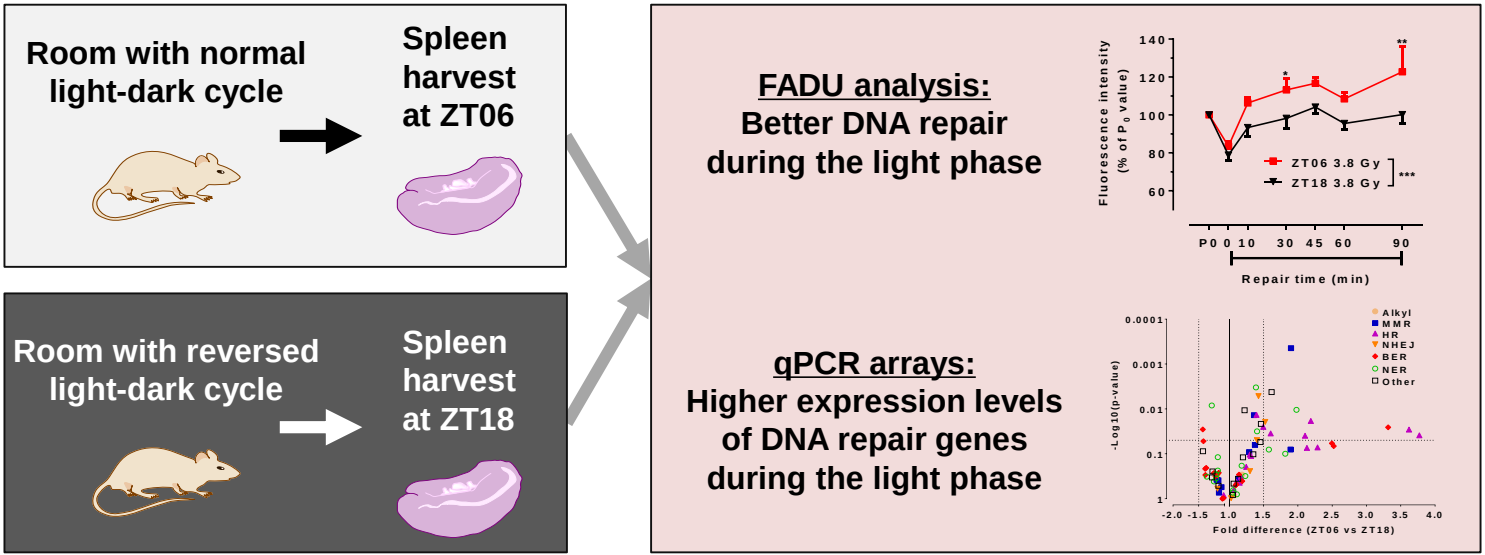

Day and night variations in the repair of ionizing-radiation-induced DNA damage in mouse splenocytes

Philipp Palombo, Maria Moreno-Villanueva, and Aswin Mangerich[*]

University of Konstanz, Molecular Toxicology Group, Department of Biology, D-78457 Konstanz, Germany

Address all correspondence to: Aswin Mangerich, Email: aswin.mangerich@uni-konstanz.de

Keywords: DNA repair, circadian rhythm, molecular clock, FADU assay, gene profiling, qPCR, ionizing radiation

Running title: Circadian differences in DNA repair in mouse splenocytes

Abbreviations: BER, base excision repair; FADU, fluorimetric detection of alkaline DNA unwinding; HR, homologous recombination; IR, ionizing radiation; LD cycle, light-dark cycle; MMR, mismatch repair; NER, nucleotide excision repair; NHEJ, non-homologous end-joining; ZT, *Zeitgeber* time

© 2015. This manuscript version is made available under the Elsevier user license
http://www.elsevier.com/open-access/userlicense/1.0/

Abstract

In mammals, biological rhythms synchronize physiological and behavioral processes to the 24-hour light-dark (LD) cycle. At the molecular level, self-sustaining processes, such as oscillations of transcription-translation feedback loops, control the circadian clock, which in turn regulates a wide variety of cellular processes, including gene expression and cell cycle progression. Furthermore, previous studies reported circadian oscillations in the repair capacity of DNA lesions specifically repaired by nucleotide excision repair (NER). However, it is so far only poorly understood if DNA repair pathways other than NER are under circadian control, in particular base excision and DNA strand break repair. In the present study, we analyzed potential day and night variations in the repair of DNA lesions induced by ionizing radiation (*i.e.*, mainly oxidative damage and DNA strand breaks) in living mouse splenocytes using a modified protocol of the automated FADU assay. Our results reveal that splenocytes isolated from mice during the light phase (ZT06) displayed higher DNA repair activity than those of the dark phase (ZT18). As analyzed by highly sensitive and accurate qPCR arrays, these alterations were accompanied by significant differences in expression profiles of genes involved in the circadian clock and DNA repair. Notably, the majority of the DNA repair genes were expressed at higher levels during the light phase (ZT06). This included genes of all major DNA repair pathways with the strongest differences observed for genes of base excision and DNA double strand break repair. In conclusion, here we provide novel evidence that mouse splenocytes exhibit significant differences in the repair of IR-induced DNA damage during the LD cycle, both on a functional and on a gene expression level. It will be interesting to test if these findings could be exploited for therapeutic purposes, e.g. time-of-the-day-specific application of DNA-damaging treatments used against blood malignancies.

1. Introduction

As a result of the rotation of the earth, most organisms developed biological rhythms that synchronize physiological and behavioral processes to the 24-hour light-dark (LD) cycle, including the sleep-wake cycle, body temperature, metabolism, and stress response. The disruption of such circadian rhythms can profoundly contribute to disease development such as sleep disorders, metabolic and neurological diseases, as well as cancer formation. On the other hand, detailed knowledge about circadian rhythms can support optimal timing of medication to enhance efficacy and reduce side-effects of pharmacological treatments, *i.e.*, chronopharmacology [1]. The regulation of circadian rhythms in mammals is organized in an hierarchical manner [2]. On the organismic level, the suprachiasmatic nucleus (SCN) of the hypothalamus is the main pacemaker. It receives its input directly from external light from the retina, which acts as the main *Zeitgeber* ('time giver') and synchronizes biological rhythms to the 24-h LD cycle. Additional peripheral clocks exist in most tissues, such as liver and muscle. They are synchronized by the SCN, however oscillate in an autonomous manner [2].

On the molecular level, sophisticated self-sustained mechanisms have evolved to control circadian rhythms [2]. One of the most fundamental time keeping mechanisms comprises multiple interacting transcription-translation feedback loops (TTFL). In mammals the transcription factors BMAL1/2 dimerize with CLOCK or NPAS2, which drive the expression of *Period* (*Per1-3*) and *Cryptochrome* (*Cry1/2*) genes via binding to E-box promoter elements [3]. At a certain threshold PER and CRY complexes translocate to the nucleus, where they inhibit the transcriptional activity of BMAL and CLOCK, and in consequence, the expression of *Per* and *Cry* genes [3]. Following phosphorylation by casein kinases (CKIε) the PER/CRY complexes are ubiquitylated and degraded by the proteasome, thereby reactivating *Clock* and *Bmal* expression. This cycle repeats itself every 24 h and is stabilized

by additional intertwined feedback loops [3]. For example, the retinoic acid receptor-related orphan receptors, REV-ERBα/β and ROR, interact with enhancer elements on the *Bmal1* promoter to inhibit or activate transcription, respectively. The BMAL/CLOCK complex, in turn, directly acts on the REV-ERB transcription, thereby forming an additional fine-tuning loop [3]. Apart from controlling expression of circadian genes, core circadian transcription factors regulate the rhythmic transcription a plethora of other genes, *i.e.*, clock-controlled genes (CCG), including 'downstream' cascade transcription factors. Several genome-wide microarray and RNA sequencing approaches have shown that the expression of 10-20% of all genes is under circadian control, however, the spectrum of genes is largely tissue specific [4-8]. Besides TTFLs, additional time-keeping mechanisms exist, such as self-sustained oscillations in post-translational modifications, epigenetic states, metabolic processes, and the redox status [3, 9].

In addition to their circadian function, clock factors are involved in other cellular processes such as metabolic processes, cell cycle regulation, and DNA repair [10]. The presence of a photolyase domain in cryptochromes suggests that the molecular clock co-evolved with DNA repair mechanisms during evolution [9, 11]. Although in mammals cryptochromes lost photolyase activity [9], some studies have demonstrated an interplay between circadian and DNA repair mechanisms in mice. At least six major DNA repair pathways exist in mammals, *i.e.* (*i*) direct repair of alkylated bases by enzymes such as O^6-methyl guanine methyltransferase (MGMT); (*ii*) repair of small base adducts by base excision repair (BER); (*iii*) repair of bulky base adducts by nucleotide excision repair (NER); (*iv*) correction of mispaired bases by mismatch repair (MMR); and (*v*) the repair of DNA double strand break (DSB) by homologous recombination (HR) or non-homologous end joining (NHEJ) [12]. Direct connections of the circadian clock with mammalian DNA repair systems have been established lately. For example, factors of the core clock itself, such as PER1, CLOCK, and CRY1, are directly involved in mechanisms of genome maintenance [13-15]. Moreover,

indirect regulatory functions have been established, in particular in the circadian regulation of NER and DNA damage signaling [10, 16-18]. Kang *et al.* demonstrated that the NER capacity oscillates in various mouse organs, such as brain, liver, and skin, but not in testis [19-21]. These studies suggested that the transcriptional as well as post-transcriptional regulation of XPA is key to the overall oscillation of NER. Concerning DNA damage signaling, the TIM (timeless) protein, which is required for a robust circadian regulation in the mouse, appears to be of critical importance [17, 22]. Thus, TIM interacts with various DNA damage response (DDR) factors, such as ATR and CHK1 as well as with circadian factors such as CRY2 [17, 22]. Functionally, TIM is a replication fork-associated factor that is required for proper ATR-dependent CHK1 and ATM-dependent CHK2 signaling [22, 23]. Consistently, reduction in TIM and its associated partner TIPIN render cells sensitive to DNA damage treatments [24]. This regulation appears to be reciprocal, since ATM and ATR phosphorylate TIM upon DNA damage [25]. In general, TIM connects the circadian clock with the DDR and cell cycle control. In terms of cell cycle control, it has been reported that p20 and p21 are clock-controlled factors, and consequently G1/S transition is partly clock-dependent [17, 26-28]. Similarly, the circadian clock has been implicated in G2/M checkpoint transition [17, 29, 30]. The WEE1 kinase, which is responsible for regulating the cyclin B1/CDC2 complex and subsequent entry into mitosis, is directly under circadian control and appears to act as a key factor in circadian-controlled G2/M transition [29]. In addition, other cell cycle regulating factors, such as c-Myc, Cyclin D1, Cyclin A, Cyclin B1 and CDC2, show circadian oscillations, indicating that the circadian clock and cell cycle are closely coupled biological circuits [17, 31]. The significance of these results on a molecular level is impressively demonstrated by the findings that the induction of skin cancer in the mouse is time-of-the-day dependent [21], and that environmental disruption of the circadian clock in humans leads to a higher cancer incidence [32].

Despite the potential impact of circadian variations in DNA repair on human health, at present, it is only poorly understood if DNA repair pathways other than NER, in particular BER and DSBR, show circadian variations. To address this question, in the present study, we analyzed if day and night differences in the repair of DNA lesion induced by ionizing radiation (IR) exist in mouse splenocytes. Splenocytes are mainly composed of immune cells, *i.e.*, lymphoid cells [33] and this tissue has so far been only poorly characterized with regards to circadian differences in DNA repair. As expected, mouse splenocytes displayed significantly different transcript levels of genes related to the circadian clock at the light (ZT06) vs. the dark (ZT18) phase. Using a modified protocol of the automated FADU assay, we demonstrated that DNA repair exhibits significant day and night variations, showing higher repair activities during the light phase. Interestingly, these differences were accompanied by significant variations in the expression levels of DNA repair genes of all major DNA repair pathways, with most of the regulated genes being up-regulated during the light phase. Our results indicate that DNA repair activities of splenocytes show significant differences during the 24 h LD cycle, which may be exploited in time-of-the-day-optimized application of DNA-damaging therapies to treat lymphoid malignancies.

2. Material and Methods

Mouse husbandry and tissue collection. All experiments were performed according to national guidelines and approved by local veterinary authorities (*Regierungspräsidium* Freiburg, Germany). Mice were housed in the central animal care facility of the University of Konstanz, in individually ventilated cages (IVC) and fed *ad libitum* on a normal fat diet (No. 3800; Kliba Nafag, Kaiseraugst, Switzerland). Pathogen and parasite-free status was verified periodically by microbiological and serological health monitoring in accordance with FELASA recommendations performed by MFD Diagnostics (Wendelsheim, Germany). All

mice were housed in a 12 h light/12 h dark cycle. One group of mice (termed "ZT06") were housed in a room with light on at 7 AM (normal LD cycle). A separate mouse colony (termed "ZT18") was established by an initial 12-h light shift in a separate room (light on at 7 PM, reversed LD cycle) (**Figure 1**). These founder animals were adapted to the reverse LD cycle for >3 weeks and then interbred to establish a colony that is born into the reverse LD cycle. This experimental setup was necessary in order to isolate spleens concomitantly at the light and the dark phase in order to obtain freshly isolated splenocytes for a side-by-side comparison of DNA repair capacities using the FADU assay. Mice were killed by CO_2 inhalation. Immediately afterwards, spleens were removed, one part of the organ was immediately submerged in RNA later solution (Qiagen), and stored at -80° for further analysis. The other part was incubated in ice-cold PBS and prepared for FADU analysis.

Isolation of splenocytes. Isolation of primary splenocytes was performed on ice or at 4°C according to a previously described procedure [33]. Briefly, spleens were cut in small pieces and then expelled through a 100-µm nylon mesh cell strainer. After washing the cell strainer with 10 ml DMEM and cells were pelleted at 800× *g* for 5 min at 4°C. The cell pellet was resuspended in 1 ml ACK lysis buffer (150 mM NH_4Cl, 10 mM $KHCO_3$, 120 µM EDTA) and incubated for 5 min on ice to lyse erythrocytes. Subsequently, lysis was stopped by adding 9 ml of DMEM, cells were pelleted at 800× *g* for 5 min at 4°C, resuspended in DMEM, and incubated for 30 min at 37°C in a regular CO_2-controlled incubator to allow cells to recover from isolation. Cell numbers were determined using a Casy Cell Counter TT (Roche).

DNA repair analysis by FADU assay. FADU analysis was performed as described previously, with adaptations to optimize conditions to measure DNA damage and repair in mouse splenocytes [34, 35]. Experiments were performed with 5 mice per ZT group, *i.e.,* five biological replicates. For each replicate, splenocytes from two mice, *i.e.*, one mouse

from ZT06 and ZT18, respectively, were isolated side-by-side. For each FADU sample (*i.e.*, T, P0, R1-6) 7.5×10^5 cells were resuspended in 100 µl DMEM. Cells were irradiated at doses as indicated using an X-ray generator from CHF Müller (Hamburg, Germany). The irradiation parameters were the following: 70 keV energy, 1.25-mm aluminium filter, and 9.4 mA current. Afterwards, samples T and P_0 were kept on ice, whereas R_x samples were incubated at 37°C in a water bath for 0, 10, 20, 30, 45, 60 or 90 min to allow DNA repair to occur. After these time points, samples were put on ice to stop DNA repair, were subsequently transferred to a modified Tecan pipetting robot as described previously [34, 35], and an automated pipetting program was started: First, 900 µl of ice cold suspension buffer (0.25 M myo-inositol, 10 mM Na_2PO_3, 1 mM MgCl, pH 7.4) were added to the 100 µl cell suspension. Then, 70 µl of the diluted cell suspension were transferred to three wells of a 96-well plate (cooled to 0°C). Next 70 µl of lysis buffer [9 M urea, 10 mM NaOH, 2.5 mM cyclohexyl-diaminetetraacetate, 0.1% (w/v) SDS] were added to each well and incubated for 12 min at 0°C. Afterwards, 140 µl neutralization buffer [1 M D-(+)-glucose-monohydrate, 14 mM β-mercaptoethanol] were added only to T samples. Then, 70 µl of ice-cold alkali buffer [42.5% (v/v) FADU lysis buffer, 0.2 M NaOH] were added to each well and incubated for 5 min at 0°C. Next, the 96-well plate was heated to 30°C and incubated for 30 min to allow unwinding of DNA. Afterwards, the 96-well plate was cooled down to 18°C and incubated for another 30 min, before 140 µl of neutralization buffer were added to each well except for the T samples. Finally, 156 µl diluted SYBR Green (1:8,333 in H2O) were added to each well and fluorescence intensity was measured by a FL600 microplate fluorescence reader (Bio-TEK Instruments) using an excitation and emission wavelength of 492/520 nm, respectively.

Targeted gene expression profiling by qPCR analysis. Gene expression profiling was carried out using RT^2 Profiler PCR arrays [Qiagen, mouse circadian rhythms array (PAMM153Z)

and mouse DNA repair array (PAMM-042Z)] on a Biorad CFX Connect system. All steps were performed according to the manufacture's instructions with the following specifications. Experiments were performed with ≥5 mice per ZT group, *i.e.*, ≥5 biological replicates. RNA-Later-conserved tissue (15-20 mg) was homogenized using a rotor-stator homogenizer and RNA prepared using the RNeasy Mini kit (Qiagen). RNA quantity and quality was analyzed at 260/280 nm. Reverse transcription was performed with 2 µg of total RNA using the RT^2 First Strand kit (Qiagen). Genomic DNA and reverse transcription controls were included in each PCR run to check for genomic DNA contaminations and impurities in RNA samples that may affect reverse transcription, respectively. All experiments met quality control standards as recommended by the manufacturer. C_t values were normalized to five different control genes (*Actb*, *B2m*, *Gapdh*, *Gusb*, *Hsp90ab1*) for comparison of mice in different circadian phases. Data were analyzed using the PCR Array Data Analysis Web Portal (www.sabiosciences.com/pcrarraydataanalysis.php) according to the $\Delta\Delta C_t$ method.

Multivariate and statistical data analysis. Multivariate data analysis was carried out using the Multibase2015 Excel Add-in. Hierarchical cluster analysis (HCA) was performed using the furthest neighbor method. Genes that were expressed at significant different levels at ZT06 vs. ZT18 were included in the principal component analysis (PCA). Statistical data analysis was performed using the PCR Array Data Analysis Web Portal (www.sabiosciences.com/pcrarraydataanalysis.php) and GraphPad Prism 6. P values < 0.05 were considered statistically significant. STRING (Search Tool for the Retrieval of Interacting Genes/Proteins) database [36] was used to visualize known interactions among genes that showed significant differences in transcript levels in qPCR analysis.

3. Results

To study potential differences in repair activities of mouse splenocytes at different circadian time points it was essential to prepare samples for DNA repair analysis using the automated FADU assay at different *Zeitgeber* times (ZT) in parallel. For this reason, we established a mouse colony with a 12-h shift in the light-dark cycle (reversed LD cycle) (**Figure 1**). Mice of the normal LD cycle (light on at 7 am) and the reversed LD cycle (light on at 7 pm) were housed in separate rooms that only differed in the LD cycle, but provided otherwise identical housing conditions (*i.e.*, temperature, litter, food and air supply, room dimensions, etc.). To ensure full adaptation to the respective ZT, only mice that were born into their respective LD cycle were included in experiments. Since NER was reported to show significant differences at ZT06 and ZT18 in mouse brain [19], we chose these ZTs as representative times in the present study as well.

3.1 Targeted expression profiling of genes related to circadian rhythm

To validate that the two groups of mice indeed differed in their ZTs, we performed targeted expression analysis via qPCR arrays on a representative set of 84 genes that are involved in circadian regulation (http://www.sabiosciences.com/ rt_pcr_product/HTML/PAMM-153A.html). In contrast to hybridization-based microarray techniques and RNA sequencing, which allow genome-wide coverage, qPCR analysis is considered to be more quantitative and also suitable to reveal subtle changes in transcript levels [37]. From the 84 circadian genes analyzed, 18 showed significantly different transcript levels between the two groups (21.4% in total; 9.5% lower and 11.5% higher levels at ZT06, respectively). When analyzing the whole transcriptional data set in a hierarchical cluster analysis, a clear separation of mice at ZT06 and ZT18 became obvious, verifying that the two groups are indeed in different circadian states (**Figure 2 A**). Among the genes that were significantly regulated, were factors of the core clock machinery, such as *Per2*, *Per3*, *Cry1*, *Tim* (*Timeless*), *Fbxl3*, *Npas2*, and *Nr1d1* (REV-ERBα), as well as downstream circadian-regulated transcription factors

such as *Ppara*, *Hlf*, *Rorc*, *Rorb*, *Stat5a*, *Wee*1 (**Figure 2B**). Principle components analysis (PCA) of factors that showed significant differences only, revealed that mice from the two groups clearly separated along the first and the second PC, with the first PC accounting for 55.6% of the total variability, and the second PC for 14.9% of the variability (**Figure 2C**). As it is evident from the loadings plot (**Figure 2C**), the top ten factors that accounted for the largest portion of variance among the two groups were *Cry1*, *Stat5a*, *Npas2*, *Per3*, *Ppara*, *Fbxl3*, *Csnk1a1*, *Tim* (*Timeless*), *Hebp1*, and *Wee1*. In summary, these results verified that the two groups of mice are indeed in different circadian states and therefore represent a suitable model for side-by-side comparison of day and night differences in biological processes.

3.2 Adaptation of the FADU assay to analyze DNA repair in mouse splenocytes

As we reported previously, the automated FADU assay represents a rapid and reliable method to analyze DNA strand break levels and DNA repair kinetics in human suspension cells, *i.e.,* PBMCs and Jurkat cells [34, 35, 38]. As discussed in [34], this assay represents an equivalent alternative to the comet assay. In the present study, we further adapted and optimized a protocol that previously proved suitable to measure repair kinetics in mouse splenocytes [39]. The principle of the method is based on the time-dependent alkaline unwinding of double-stranded DNA and subsequent detection of SYBR Green-derived fluorescence intensity, which correlates with the amount of double stranded DNA and is inversely proportional to the amount of DNA strand breaks. The assay includes the following working steps (**Figure 3A**): (*i*) After cell preparation, (*ii*) DNA damage is induced by x-ray irradiation. (*iii*) Cells are incubated at 37°C for defined periods to allow DNA repair. (*iv-v*) Cells are transferred to a 96-well plate by an automated liquid handling device and are lysed. (*vi*) Lysates are treated with an alkaline solution to unwind double-stranded DNA. (*vii*) DNA unwinding is stopped by sample neutralization. (*viii-x*) SYBR Green is added to determine

the remaining amount of the double stranded DNA via fluorescence read-out, and data are analyzed (*xi*). Working steps (*iv*) to (ix) are performed in an automated manner by a liquid handling device in a 96-well plate format. The following sample types are included in each experiment: Cells of T samples were not irradiated. To these samples, neutralization buffer was added before addition of unwinding buffer, thus unwinding did not take place and fluorescence readout from T samples represents the total amount of DNA. Like T samples, P_0 samples were not irradiated, but in this case alkaline DNA unwinding takes place. Thus, only the DNA sites that are accessible by physiological causes (replication forks, chromosome ends, endogenous damage, etc.) are starting points for DNA unwinding. The ratio between T and P_0 samples gives a measure for the amount of endogenous DNA strand breaks. R_x samples were irradiated to induce DNA damage. Afterwards they are incubated for a defined period of time (x min) at 37°C to allow DNA repair. In order to adapt the original FADU protocol for the usage on mouse splenocytes, several modifications were necessary. In particular, the unwinding time was reduced to account for the higher sensitivity of mouse cells compared to human cells to alkaline unwinding (for details please refer to the Material and Methods section). Using this modified protocol, X-ray irradiation of cells with doses of 1.5-9 Gy resulted in a near-linear dose-dependent induction of DNA strand breaks in splenocytes (**Figure 3B).** Furthermore, these strand breaks were efficiently repaired within 1 h after damage induction (**Figure 3C**). In summary, we provide a detailed report and validation of an adapted protocol of the automated FADU assay to analyze DNA strand breaks and DNA repair in living mouse splenocytes.

3.3 DNA repair analysis by FADU

To assess if splenocytes at different ZTs differ in their load of basal strand breaks and DNA repair activities, we performed FADU measurements with freshly isolated splenocytes from mice at ZT06 and ZT18 in side-by-side comparisons. As it is evident from **Figure 4A**, basal

levels of strand breaks did not differ between the two groups. When analyzing damage levels immediately after irradiation with a medium (3.8 Gy) and a high dose (6 Gy) dose, there was a tendency for higher damage levels in mice of the ZT18 group. Despite the fact that this difference did not reach statistical significance (**Figure 4 B**), it may be caused by circadian differences in the oxidative state of the cells, as reported previously for mouse skin cells [40]. Importantly, repair kinetics over a period of 90 min revealed that mice of the ZT06 group displayed significantly faster and higher repair activities at both IR doses tested (**Figure 4C-D**). Repair activity was up to 20% higher in ZT06 compared to ZT18 samples. The finding that this effect was more pronounced in the medium dose range of 3.8 Gy points to the possibility that at higher doses of 6 Gy, cellular mechanisms apart from DNA repair, such as cell cycle arrest and apoptosis induction, become more predominant cellular stress responses. Interestingly, we consistently observed a transient drop in fluorescence intensities around 60 min after irradiation. This drop was also observed previously in human cells [38], and can be presumably attributed to the occurrence of DNA strand breaks as DNA repair intermediates. In summary, these results indicate that mouse splenocytes exhibit significantly enhanced DNA repair activities during the light phase of the day.

3.4 Targeted gene expression analysis of DNA repair genes

To analyze if differences in DNA repair are accompanied by changes in expression of DNA repair genes, we performed qPCR analyses on a representative set of 84 DNA repair genes (http://www.sabiosciences.com/rt_pcr_product/HTML/PAMM-042A.html). From the 84 genes analyzed, 23 showed significantly different transcript levels between the two groups (27.4% in total; 3.5% lower and 23.8% higher levels at ZT06, respectively). When analyzing the complete data set in a hierarchical cluster analysis, mice of the ZT06 and ZT18 groups separate from each other with the exception of one mouse of the ZT06 group (**Figure 5A**). Genes that were significantly regulated included factors of all major DNA repair pathways

including MMR, BER, NER, HR, and NHJE. The strongest differences were observed for genes of BER (*Neil3*, 3.3-fold difference) and HR (*Brca1* and *Brca2*, >3.5 fold difference), and the most significant ones for genes of the MMR (*Pms2*) and NER (*Xpa*) (**Figure 5B**). When performing a PCA of factors that showed statistical significant differences only, mice from the two groups clearly separated along the first as well as the second PC, with the first PC accounting for 64.4% of the total variability, and the second PC for 14% of the variability (**Figure 5C**). As it is evident from the loadings plot (**Figure 5C**), the top ten factors that accounted for the largest portion of variance among the two groups were *Atr, Msh3, Xpa, Xrcc5, Parp2, Pold3, Brac1, Brca2, Neil3,* and *Rad51.* In summary, these results suggest that higher DNA repair activity in mouse splenocytes during the light phase is accompanied by higher expression levels of DNA repair factors, including those that are involved in the repair of IR-induced DNA damage, *i.e.*, oxidative and single strand break lesions as well as double strand breaks.

4. Discussion

Circadian regulation of DNA repair has recently attracted considerable attention due to its potential significance in cancer development, chronopharmacology, and risk assessment of genotoxic insults [1, 17, 32]. Specifically, NER has been extensively studied in mouse organs such as brain, liver, muscle, skin, and testis by using cell-lysate-based excision repair assays or by monitoring the removal kinetics of UV-induced DNA photoadducts [19-21]. In contrast, potential day and night differences in oxidative and strand break repair are so far only poorly understood. To address this question, we analyzed DNA strand break repair in murine spleen-derived lymphoid cells (*i.e.*, splenocytes) using an automated version of the FADU assay [34, 35, 38, 39]. Our study revealed significant faster and more efficient repair of IR-induced DNA lesions during the light phase (ZT06) compared to the dark phase (ZT18)

of the day. Importantly, this functional difference in DNA repair was accompanied by higher expression of DNA repair genes involved in all major DNA repair pathways.

In preparation of this study, we established a mouse colony with a 12-h shift in the LD cycle. Except for this shift, the colony in the reversed LD cycle was housed under identical conditions compared to the mice in a normal LD cycle. To verify that the two groups of mice are indeed in different circadian states, we performed a qPCR array analysis of genes involved in circadian regulation. This analysis demonstrated differential regulation of central clock genes between the two groups of mice. Thus, negative regulators of the circadian clock, such as *Per2*, *Per3*, and *Cry1* showed lower levels at ZT06, whereas positive regulators, such as *Npas2,* showed higher expression levels at ZT06. Moreover, other central clock factors [3], such as *Nr1d1* (REV-ERBα), *Ror* transcripts, and the E3 ubiquitin ligase *Fbxl3*, displayed highly significant differences between the two groups. It is noteworthy that the different expression levels in circadian factors are largely in accordance to previous reports that analyzed transcript levels of core clock factors in mouse spleens [41, 42]. Importantly, *Wee1* and *Tim* (timeless), two factors that were previously shown to connect the circadian clock with cell cycle regulation and DNA damage response mechanisms [17, 22-25, 29], were also expressed at significantly different levels during the light and the dark phase. On the other hand, the fact that some clock factors, such as *Clock*, *Bmal*, or *Per1,* did not show any significant differential expression can be attributed to the fact that this study focused on the analysis of two distinct circadian time points, *i.e.*, ZT06 and ZT18. Therefore, we cannot exclude that some genes among the ones that did not show expression differences in this study, still are under circadian control in mouse splenocytes; however, this may only become obvious at other circadian time points. Alternatively, these factors may be not as robustly regulated in the spleen as it was observed in other mouse organs [3]. The latter possibility is supported by studies that showed that CLOCK functions can be taken over by NPAS2 in specific tissues [43-45] and that BMAL1 and PER1 do not consistently display

circadian oscillations in spleen-derived cells [42]. Overall, our results support a growing body of evidence that the immune system, in general, and immune cells of the spleen, in particular, are under circadian control [42, 46-48]. In summary, we established mouse colonies with a normal and a reversed LD cycle, respectively, and verified a shift in circadian rhythmicity on a molecular level by targeted gene expression analysis. We chose this experimental set-up in order to compare DNA repair activities in cells of different ZTs side by side, as the FADU assay relies on the usage of freshly isolated living cells.

Our findings of higher DNA repair activities for IR-induced DNA damage in mouse splenocytes during the light phase (ZT06) resemble findings observed for NER in other mouse organs [19-21], indicating that DNA repair shows variations during the LD cycle. For example, Sancar and colleagues detected higher NER activities in brain and liver extracts at ZT06 compared to ZT18 [19, 20]. Furthermore, the same group reported more efficient removal of UV-induced DNA damage in the skin during the light (ZT09) compared to the dark phase (ZT21) [21]. These studies revealed that circadian oscillation in XPA mRNA and proteins levels is the rate-limiting factor for NER activity in these tissues [19-21]. Of note, our qPCR analysis also detected Xpa transcripts at significantly higher levels at ZT06 compared to ZT18 in mouse splenocytes. Our study significantly extends the findings by Sancar and colleagues by demonstrating that not only NER-substrates, but also IR-induced DNA damage is more efficiently repaired during the light phase of the day. In contrast to mouse skin, in which lower levels of DNA damage, *i.e.* UV-photoproducts and γH2A.x-postive cells, were reported during the light phase [40], we did not observe any difference in basal levels of DNA strand breaks in splenocytes. This may be related to a higher burden of exogenously-induced DNA damage in the mouse skin (e.g., by UV light) or to organ and damage-specific differences. Our targeted gene expression analysis on DNA repair factors revealed that factors of all major DNA repair pathways show differential expression patterns, further supporting the notion that DNA repair in general is under circadian control in the

spleen. Interestingly, DNA repair turned up as one of four major gene expression clusters that are under circadian control in rat liver [49]. Furthermore, according to the circadian expression profiles data base (CircaDB) [50], several of the transcipts that showed differential regulation in the present study, such as Brca1/2, Rad51, Rad18, Xrcc2, Pms2, and XPA, are also under circadian control in other mouse tissues. Strikingly, our results reveal that factors of repair mechanisms, such as BER and HR, which are responsible for the repair of IR-induced damage, displayed the most prominent differences. The notion that strand break repair is under circadian control is further supported by previous studies demonstrating that TIM is involved in ATM/ATR-dependent strand break signaling [22-25]. Consistently, cells depleted in the TIM-associated factor Tipin showed higher sensitivity to IR [24]. Further evidence for circadian control of strand break repair stems from indirect evidence showing that IR caused more hair loss in mice, when administered in the morning compared with the evening [40]. Several studies came to the conclusion that DNA repair is antiphasic to DNA replication [21, 30, 40], indicating that cell cycle control and DNA repair represent interconnected circadian-dependent biological circuits. As it is obvious from a STRING database analysis [36] of all factors that showed significantly different expression levels in our study, particularly TIM and WEE1 appear to connect DNA repair with the molecular clock **(Figure 6)**. This network provides a foundation for follow-up studies to analyze the mechanistic basis for the day and night differences in DNA repair activities in splenocytes and other tissues in mice as well as in humans. In particular, the detailed analysis of BRCA1/2 and other factors of HR will be of critical importance, considering the significance of this DNA repair pathway in carcinogenesis and as a therapeutic target [51]. In this regard, it is interesting to note that protein levels of HR factors, such as BRCA1 and RAD51, can be controlled by transcriptional regulation [52, 53]. Specifically, a study in human cells, which is unrelated to circadian biology, demonstrated that changes in the NAD^+/NADH ratio can regulate *BRCA1* expression levels via changes in histone acetylation [52, 53]. It is tempting

to speculate that circadian oscillations in intracellular NAD^+ levels as described previously [54], may induce changes in *Brca1* gene expression as observed in our study.

5. Conclusions

In conclusion, here we provide evidence for a day and night difference in the repair of IR-induced DNA damage in the mouse spleen. Future studies need to clarify if analogous daytime-specific differences in DNA repair exist in humans. A study by Marchenay *et al.* supported this notion, as these authors suggested that DNA dealkylation repair activity displays circadian variation in human PBMCs [55]. If this holds true for other DNA repair pathways, this could have important implications in terms of risk assessment of genotoxic exposures (e.g., UV-damage by sunlight exposure) and diseases development due to disrupted circadian rhythms (e.g., higher cancer risk in shift workers). Strong evidence for the hypothesis that circadian regulation of DNA repair can be causal in cancer development is given by findings that UV-induced skin cancer formation in the mouse is dependent on the daytime of irradiation [21] and by epidemiological findings suggesting that disruption of the circadian clock increases the risk of cancer development in humans [32, 56]. Furthermore, considering the central importance of DNA-damaging agents in cancer therapy, it is obvious that a detailed understanding of circadian regulation of DNA repair and cell cycle control is of paramount importance in clinical pharmacology [1, 16, 57, 58]. Several studies provided evidence that the efficacy and side-effects of DNA-damaging anticancer therapies are day-time dependent [59].

Author contributions

AM designed the study. PP and AM designed experiments. PP performed experiments. PP and AM analyzed data. MMV provided essential scientific input and technical expertise. PP and MMV edited the manuscript. AM wrote the manuscript.

Acknowledgments

We thank Alexander Bürkle for valuable discussions and critical reading of the manuscript, Jennifer Baur for advice in statistical analysis, and Shuran Yu for contributions during her practical course work. This work was supported by the *Zukunftskolleg* Konstanz (Independent Research Start-up Grant to AM) and the University of Konstanz (*Ausschuss für Forschungsfragen,* AFF).

References:

[1] R. Dallmann, S.A. Brown, F. Gachon, Chronopharmacology: New Insights and Therapeutic Implications, Annual Review of Pharmacology and Toxicology, 54 (2014) null.
[2] J.A. Ripperger, C. Jud, U. Albrecht, The daily rhythm of mice, FEBS Lett, 585 (2011) 1384-1392.
[3] I. Robinson, A.B. Reddy, Molecular mechanisms of the circadian clockwork in mammals, FEBS Letters, 588 (2014) 2477-2483.
[4] K.F. Storch, O. Lipan, I. Leykin, N. Viswanathan, F.C. Davis, W.H. Wong, C.J. Weitz, Extensive and divergent circadian gene expression in liver and heart, Nature, 417 (2002) 78-83.
[5] N. Koike, S.H. Yoo, H.C. Huang, V. Kumar, C. Lee, T.K. Kim, J.S. Takahashi, Transcriptional architecture and chromatin landscape of the core circadian clock in mammals, Science, 338 (2012) 349-354.
[6] B.H. Miller, E.L. McDearmon, S. Panda, K.R. Hayes, J. Zhang, J.L. Andrews, M.P. Antoch, J.R. Walker, K.A. Esser, J.B. Hogenesch, J.S. Takahashi, Circadian and CLOCK-controlled regulation of the mouse transcriptome and cell proliferation, Proc Natl Acad Sci U S A, 104 (2007) 3342-3347.
[7] K. Oishi, K. Miyazaki, K. Kadota, R. Kikuno, T. Nagase, G. Atsumi, N. Ohkura, T. Azama, M. Mesaki, S. Yukimasa, H. Kobayashi, C. Iitaka, T. Umehara, M. Horikoshi, T. Kudo, Y. Shimizu, M. Yano, M. Monden, K. Machida, J. Matsuda, S. Horie, T. Todo, N. Ishida, Genome-wide expression analysis of mouse liver reveals CLOCK-regulated circadian output genes, J Biol Chem, 278 (2003) 41519-41527.
[8] S. Panda, M.P. Antoch, B.H. Miller, A.I. Su, A.B. Schook, M. Straume, P.G. Schultz, S.A. Kay, J.S. Takahashi, J.B. Hogenesch, Coordinated transcription of key pathways in the mouse by the circadian clock, Cell, 109 (2002) 307-320.
[9] J. Bass, Circadian topology of metabolism, Nature, 491 (2012) 348-356.
[10] M.P. Antoch, R.V. Kondratov, Circadian proteins and genotoxic stress response, Circ Res, 106 (2010) 68-78.
[11] C.L. Thompson, A. Sancar, Photolyase/cryptochrome blue-light photoreceptors use photon energy to repair DNA and reset the circadian clock, Oncogene, 21 (2002) 9043-9056.
[12] J.H. Hoeijmakers, Genome maintenance mechanisms for preventing cancer, Nature, 411 (2001) 366-374.
[13] S. Gery, N. Komatsu, L. Baldjyan, A. Yu, D. Koo, H.P. Koeffler, The circadian gene per1 plays an important role in cell growth and DNA damage control in human cancer cells, Mol Cell, 22 (2006) 375-382.
[14] C. Cotta-Ramusino, E.R. McDonald, 3rd, K. Hurov, M.E. Sowa, J.W. Harper, S.J. Elledge, A DNA damage response screen identifies RHINO, a 9-1-1 and TopBP1 interacting protein required for ATR signaling, Science, 332 (2011) 1313-1317.
[15] T.-H. Kang, S.-H. Leem, Modulation of ATR-mediated DNA damage checkpoint response by cryptochrome 1, Nucleic acids research, (2014).
[16] M.P. Antoch, R.V. Kondratov, Pharmacological modulators of the circadian clock as potential therapeutic drugs: focus on genotoxic/anticancer therapy, Handb Exp Pharmacol, (2013) 289-309.
[17] S. Masri, M. Cervantes, P. Sassone-Corsi, The circadian clock and cell cycle: interconnected biological circuits, Curr Opin Cell Biol, 25 (2013) 730-734.
[18] A. Sancar, L.A. Lindsey-Boltz, T.H. Kang, J.T. Reardon, J.H. Lee, N. Ozturk, Circadian clock control of the cellular response to DNA damage, FEBS Lett, 584 (2010) 2618-2625.
[19] T.H. Kang, J.T. Reardon, M. Kemp, A. Sancar, Circadian oscillation of nucleotide excision repair in mammalian brain, Proc Natl Acad Sci U S A, 106 (2009) 2864-2867.

[20] T.H. Kang, L.A. Lindsey-Boltz, J.T. Reardon, A. Sancar, Circadian control of XPA and excision repair of cisplatin-DNA damage by cryptochrome and HERC2 ubiquitin ligase, Proc Natl Acad Sci U S A, 107 (2010) 4890-4895.
[21] S. Gaddameedhi, C.P. Selby, W.K. Kaufmann, R.C. Smart, A. Sancar, Control of skin cancer by the circadian rhythm, Proceedings of the National Academy of Sciences, 108 (2011) 18790-18795.
[22] K. Unsal-Kacmaz, T.E. Mullen, W.K. Kaufmann, A. Sancar, Coupling of human circadian and cell cycles by the timeless protein, Mol Cell Biol, 25 (2005) 3109-3116.
[23] X. Yang, P.A. Wood, W.J. Hrushesky, Mammalian TIMELESS is required for ATM-dependent CHK2 activation and G2/M checkpoint control, J Biol Chem, 285 (2010) 3030-3034.
[24] D.M. Chou, S.J. Elledge, Tipin and Timeless form a mutually protective complex required for genotoxic stress resistance and checkpoint function, Proc Natl Acad Sci U S A, 103 (2006) 18143-18147.
[25] S. Matsuoka, B.A. Ballif, A. Smogorzewska, E.R. McDonald, 3rd, K.E. Hurov, J. Luo, C.E. Bakalarski, Z. Zhao, N. Solimini, Y. Lerenthal, Y. Shiloh, S.P. Gygi, S.J. Elledge, ATM and ATR substrate analysis reveals extensive protein networks responsive to DNA damage, Science, 316 (2007) 1160-1166.
[26] R. Laranjeiro, T.K. Tamai, E. Peyric, P. Krusche, S. Ott, D. Whitmore, Cyclin-dependent kinase inhibitor p20 controls circadian cell-cycle timing, Proc Natl Acad Sci U S A, 110 (2013) 6835-6840.
[27] A. Gréchez-Cassiau, B. Rayet, F. Guillaumond, M. Teboul, F. Delaunay, The Circadian Clock Component BMAL1 Is a Critical Regulator of p21WAF1/CIP1 Expression and Hepatocyte Proliferation, Journal of Biological Chemistry, 283 (2008) 4535-4542.
[28] J. Mullenders, A.W.M. Fabius, M. Madiredjo, R. Bernards, R.L. Beijersbergen, A Large Scale shRNA Barcode Screen Identifies the Circadian Clock Component ARNTL as Putative Regulator of the p53 Tumor Suppressor Pathway, PLoS ONE, 4 (2009) e4798.
[29] T. Matsuo, S. Yamaguchi, S. Mitsui, A. Emi, F. Shimoda, H. Okamura, Control mechanism of the circadian clock for timing of cell division in vivo, Science, 302 (2003) 255-259.
[30] M.V. Plikus, C. Vollmers, D. de la Cruz, A. Chaix, R. Ramos, S. Panda, C.M. Chuong, Local circadian clock gates cell cycle progression of transient amplifying cells during regenerative hair cycling, Proc Natl Acad Sci U S A, 110 (2013) E2106-2115.
[31] L. Fu, H. Pelicano, J. Liu, P. Huang, C. Lee, The circadian gene Period2 plays an important role in tumor suppression and DNA damage response in vivo, Cell, 111 (2002) 41-50.
[32] F.C. Kelleher, A. Rao, A. Maguire, Circadian molecular clocks and cancer, Cancer Lett, 342 (2014) 9-18.
[33] A.M. Kruisbeek, Isolation of Mouse Mononuclear Cells, in: Current Protocols in Immunology, John Wiley & Sons, Inc., 2001.
[34] M. Moreno-Villanueva, T. Eltze, D. Dressler, J. Bernhardt, C. Hirsch, P. Wick, G. von Scheven, K. Lex, A. Bürkle, The automated FADU-assay, a potential high-throughput in vitro method for early screening of DNA breakage, ALTEX, 28 (2011) 295-303.
[35] M. Moreno-Villanueva, R. Pfeiffer, T. Sindlinger, A. Leake, M. Muller, T.B. Kirkwood, A. Bürkle, A modified and automated version of the 'Fluorimetric Detection of Alkaline DNA Unwinding' method to quantify formation and repair of DNA strand breaks, BMC Biotechnol, 9 (2009) 39.
[36] A. Franceschini, D. Szklarczyk, S. Frankild, M. Kuhn, M. Simonovic, A. Roth, J. Lin, P. Minguez, P. Bork, C. von Mering, L.J. Jensen, STRING v9.1: protein-protein interaction networks, with increased coverage and integration, Nucleic Acids Res, 41 (2013) D808-815.

[37] C. Wang, B. Gong, P.R. Bushel, J. Thierry-Mieg, D. Thierry-Mieg, J. Xu, H. Fang, H. Hong, J. Shen, Z. Su, J. Meehan, X. Li, L. Yang, H. Li, P.P. Labaj, D.P. Kreil, D. Megherbi, S. Gaj, F. Caiment, J. van Delft, J. Kleinjans, A. Scherer, V. Devanarayan, J. Wang, Y. Yang, H.-R. Qian, L.J. Lancashire, M. Bessarabova, Y. Nikolsky, C. Furlanello, M. Chierici, D. Albanese, G. Jurman, S. Riccadonna, M. Filosi, R. Visintainer, K.K. Zhang, J. Li, J.-H. Hsieh, D.L. Svoboda, J.C. Fuscoe, Y. Deng, L. Shi, R.S. Paules, S.S. Auerbach, W. Tong, The concordance between RNA-seq and microarray data depends on chemical treatment and transcript abundance, Nat Biotech, 32 (2014) 926-932.
[38] J. Morath, M. Moreno-Villanueva, G. Hamuni, S. Kolassa, M. Ruf-Leuschner, M. Schauer, T. Elbert, A. Bürkle, I.T. Kolassa, Effects of Psychotherapy on DNA Strand Break Accumulation Originating from Traumatic Stress, Psychotherapy and Psychosomatics, 83 (2014) 289-297.
[39] A. Mangerich, N. Herbach, B. Hanf, A. Fischbach, O. Popp, M. Moreno-Villanueva, O.T. Bruns, A. Bürkle, Inflammatory and age-related pathologies in mice with ectopic expression of human PARP-1, Mech Ageing Dev, 131 (2010) 389-404.
[40] M. Geyfman, V. Kumar, Q. Liu, R. Ruiz, W. Gordon, F. Espitia, E. Cam, S.E. Millar, P. Smyth, A. Ihler, J.S. Takahashi, B. Andersen, Brain and muscle Arnt-like protein-1 (BMAL1) controls circadian cell proliferation and susceptibility to UVB-induced DNA damage in the epidermis, Proc Natl Acad Sci U S A, 109 (2012) 11758-11763.
[41] S. Liu, Y. Cai, R.B. Sothern, Y. Guan, P. Chan, Chronobiological analysis of circadian patterns in transcription of seven key clock genes in six peripheral tissues in mice, Chronobiol Int, 24 (2007) 793-820.
[42] A.C. Silver, A. Arjona, M.E. Hughes, M.N. Nitabach, E. Fikrig, Circadian expression of clock genes in mouse macrophages, dendritic cells, and B cells, Brain, behavior, and immunity, 26 (2012) 407-413.
[43] J.P. DeBruyne, D.R. Weaver, S.M. Reppert, CLOCK and NPAS2 have overlapping roles in the suprachiasmatic circadian clock, Nature neuroscience, 10 (2007) 543-545.
[44] C. Bertolucci, N. Cavallari, I. Colognesi, J. Aguzzi, Z. Chen, P. Caruso, A. Foa, G. Tosini, F. Bernardi, M. Pinotti, Evidence for an overlapping role of CLOCK and NPAS2 transcription factors in liver circadian oscillators, Mol Cell Biol, 28 (2008) 3070-3075.
[45] C.A. Dudley, C. Erbel-Sieler, S.J. Estill, M. Reick, P. Franken, S. Pitts, S.L. McKnight, Altered patterns of sleep and behavioral adaptability in NPAS2-deficient mice, Science, 301 (2003) 379-383.
[46] C. Scheiermann, Y. Kunisaki, P.S. Frenette, Circadian control of the immune system, Nat Rev Immunol, 13 (2013) 190-198.
[47] A.M. Curtis, M.M. Bellet, P. Sassone-Corsi, L.A. O'Neill, Circadian clock proteins and immunity, Immunity, 40 (2014) 178-186.
[48] M. Keller, J. Mazuch, U. Abraham, G.D. Eom, E.D. Herzog, H.-D. Volk, A. Kramer, B. Maier, A circadian clock in macrophages controls inflammatory immune responses, Proceedings of the National Academy of Sciences, 106 (2009) 21407-21412.
[49] T.T. Nguyen, J.S. Mattick, Q. Yang, M.A. Orman, M.G. Ierapetritou, F. Berthiaume, I.P. Androulakis, Bioinformatics analysis of transcriptional regulation of circadian genes in rat liver, BMC bioinformatics, 15 (2014) 83.
[50] A. Pizarro, K. Hayer, N.F. Lahens, J.B. Hogenesch, CircaDB: a database of mammalian circadian gene expression profiles, Nucleic Acids Res, 41 (2013) D1009-1013.
[51] N.J. Curtin, DNA repair dysregulation from cancer driver to therapeutic target, Nat Rev Cancer, 12 (2012) 801-817.
[52] L.J. Di, A.G. Fernandez, A. De Siervi, D.L. Longo, K. Gardner, Transcriptional regulation of BRCA1 expression by a metabolic switch, Nat Struct Mol Biol, 17 (2010) 1406-1413.

[53] C. Arias-Lopez, I. Lazaro-Trueba, P. Kerr, C.J. Lord, T. Dexter, M. Iravani, A. Ashworth, A. Silva, p53 modulates homologous recombination by transcriptional regulation of the RAD51 gene, EMBO Rep, 7 (2006) 219-224.
[54] Y. Nakahata, S. Sahar, G. Astarita, M. Kaluzova, P. Sassone-Corsi, Circadian control of the NAD+ salvage pathway by CLOCK-SIRT1, Science, 324 (2009) 654-657.
[55] C. Marchenay, E. Cellarier, F. Levi, C. Rolhion, F. Kwiatkowski, B. Claustrat, J.C. Madelmont, P. Chollet, Circadian variation in O6-alkylguanine-DNA alkyltransferase activity in circulating blood mononuclear cells of healthy human subjects, Int J Cancer, 91 (2001) 60-66.
[56] S. Sahar, P. Sassone-Corsi, Circadian clock and breast cancer: a molecular link, Cell Cycle, 6 (2007) 1329-1331.
[57] P.F. Innominato, F.A. Levi, G.A. Bjarnason, Chronotherapy and the molecular clock: Clinical implications in oncology, Adv Drug Deliv Rev, 62 (2010) 979-1001.
[58] K.C. Van Dycke, R.M. Nijman, P.F. Wackers, M.J. Jonker, W. Rodenburg, C.T. van Oostrom, D.C. Salvatori, T.M. Breit, H. van Steeg, M. Luijten, G.T. van der Horst, A day and night difference in the response of the hepatic transcriptome to cyclophosphamide treatment, Arch Toxicol, (2014).
[59] F. Levi, A. Okyar, S. Dulong, P.F. Innominato, J. Clairambault, Circadian timing in cancer treatments, Annu Rev Pharmacol Toxicol, 50 (2010) 377-421.

Figure legends

Figure 1. Establishment of mouse colonies and experimental design of the study. C57BL/6 mice from the general Konstanz mouse colony were housed under normal 12-h light-dark cycle. One group of mice was maintained in this cycle (ZT06), whereas a second group was subjected to an initial 12-h light shift (ZT18) to establish a parallel colony in a reversed LD cycle. Except for the 12-h shift in the LD cycle, both groups were housed under identical conditions in separate rooms. Mice were adapted for at least 3 weeks to these conditions before intercrossing and establishment of a mouse colony that was born into the reversed LD cycle. These mice were used for tissue harvesting and subsequent DNA repair and qPCR analysis. This experimental setup was chosen in order to isolate living splenocytes from both ZT conditions concomitantly for parallel analysis in the FADU assay. F1 indicates filial generation 1; FADU, fluorimetric detection of alkaline DNA unwinding; ZT, *Zeitgeber* time.

Figure 2. Targeted expression profiling of transcripts associated with circadian rhythm. RNA was isolated from spleens from six mice of each group and subjected to targeted qPCR analysis using the Circadian Rhythms qPCR array PAMM153Z (Qiagen). For a full list of all 84 genes included, please refer to SI Table 1. **A.** Hierarchical cluster analysis of expression data of all 84 genes reveals full separation of the two groups of mice according to the ZT of tissue harvest. **B.** Volcano plot indicating differences in gene expression levels at ZT06 vs ZT18. Horizontal line indicates P = 0.05 (n=6 mice per group); vertical line indicates no change in gene expression. Genes that are differentially expressed at a significant level or >1.5-fold are labeled with gene symbols. **C.** Principal component analysis (PCA) of significantly regulated genes. Left. Loadings plot showing the genes, whose expression differences account for the largest portion of variance. Right. Scores plot

showing distinctions between the two groups of mice according to their ZT status. Green and blue circles indicate mice from ZT18 and ZT06, respectively. CR indicates circadian rhythm, TR, transcription factor.

Figure 3. Establishment of a modified version of the FADU assay to analyze DNA repair capacities in living mouse splenocytes. A. Overview of the essential steps of the automated FADU assay (reprinted from [35], with permission). Automated steps are highlighted in bold. The protocol was adapted with respect to the original protocol as described in Material and Methods to meet requirements for the analysis of DNA repair in primary mouse splenocytes. For details see text. **B.** Dose-dependent induction of strand breaks by X-rays in mouse splenocytes. Fluorescence intensities in (% of P_0 values) give a measure for the amount of strand breaks in cellular DNA. **C.** Time course of DNA strand break repair in mouse splenocytes. To measure DNA repair, cells were irradiated with X-ray doses as indicated, then incubated for periods as indicated at 37°C, and subjected to automated FADU analysis. The P_0 value (100%) represents the level of Sybr Green fluorescence intensity in undamaged cells. Data represent means ± SEM ($n \geq 3$ mice per group).

Figure 4. FADU analysis for DNA damage and repair in mouse splenocytes at ZT06 and ZT18. A. Splenocytes from ZT06 and ZT18 do not show significant differences in physiological levels of DNA strand breaks. The P_0/T ratio represent the ratio of Sybr Green fluorescence intensities from non-irradiated, but otherwise normally processed samples (P_0 value) and matching samples, which were neutralized before alkaline unwinding (T value). The P_0/T ratio corresponds to the relative amount of strand break damage in non-irradiated samples. **B.** Levels of DNA strand break induction after X-ray irradiation with 3.8 and 6 Gy at ZT06 and ZT18. No statistical significant differences were observed in DNA strand break

levels between mice at ZT06 and ZT18. Statistical analysis was performed using Student's t-test **C-D.** DNA repair time courses at ZT06 and ZT18 after X-ray irradiation with 3.8 Gy and 6 Gy. Statistical analysis was performed using Two-Way ANOVA testing. Data represent means ± SEM (n=5 mice per group). * P<0.05, ** P<0.01, *** P<0.001. n.s. indicates non-significant.

Figure 5. Targeted expression profiling of transcripts associated with DNA repair. RNA was isolated from spleens from six mice of each group and subjected to targeted qPCR analysis using the DNA Repair qPCR array PAMM-042Z (Qiagen). Gene expression data from one mouse was not obtained during qPCR analysis for technical reasons. For a full list of all 84 genes included, please refer to SI Table 2. **A.** Hierarchical cluster analysis of expression data of all 84 genes reveals separation of the two groups of mice according to the ZT of tissue harvest, with the exception of one mouse of ZT06, which clustered near to ZT18 mice. **B.** Volcano plot indicating differences in gene expression levels at ZT06 vs ZT18. Horizontal line indicates P = 0.05 (n=5-6 mice per group); vertical line indicates no change in gene expression. Genes that are differentially expressed at a significant level or >1.5-fold are labeled with gene symbols. **C.** Principal component analysis (PCA) of significantly regulated genes. Left. Loading plot showing the genes, whose expression differences account for the largest portion of variance. Right. Scores plot showing distinctions between the two groups of mice according to their ZT status. Green and blue circles indicate mice from ZT18 and ZT06, respectively. 'Alkyl' indicates DNA repair by direct removal of alkyl groups; BER, base excision repair, MMR, mismatch repair, NER, nucleotide excision repair, NHEJ, non homologous end joining, HR, homologous recombination.

Figure 6. STRING interaction analysis of factors that displayed significantly different expression levels in qPCR array analysis. STRING generates a network based on

experimental and predicted interaction information; stronger associations between genes/proteins are represented by thicker lines [36]. Colors according to MCL cluster analysis; DNA repair factors turned up in yellow, factors involved in circadian regulation in red. Interactions between the two groups are known or predicted to be mediated by WEE1, Timeless (TIM), and FBXL3.

Figure 1

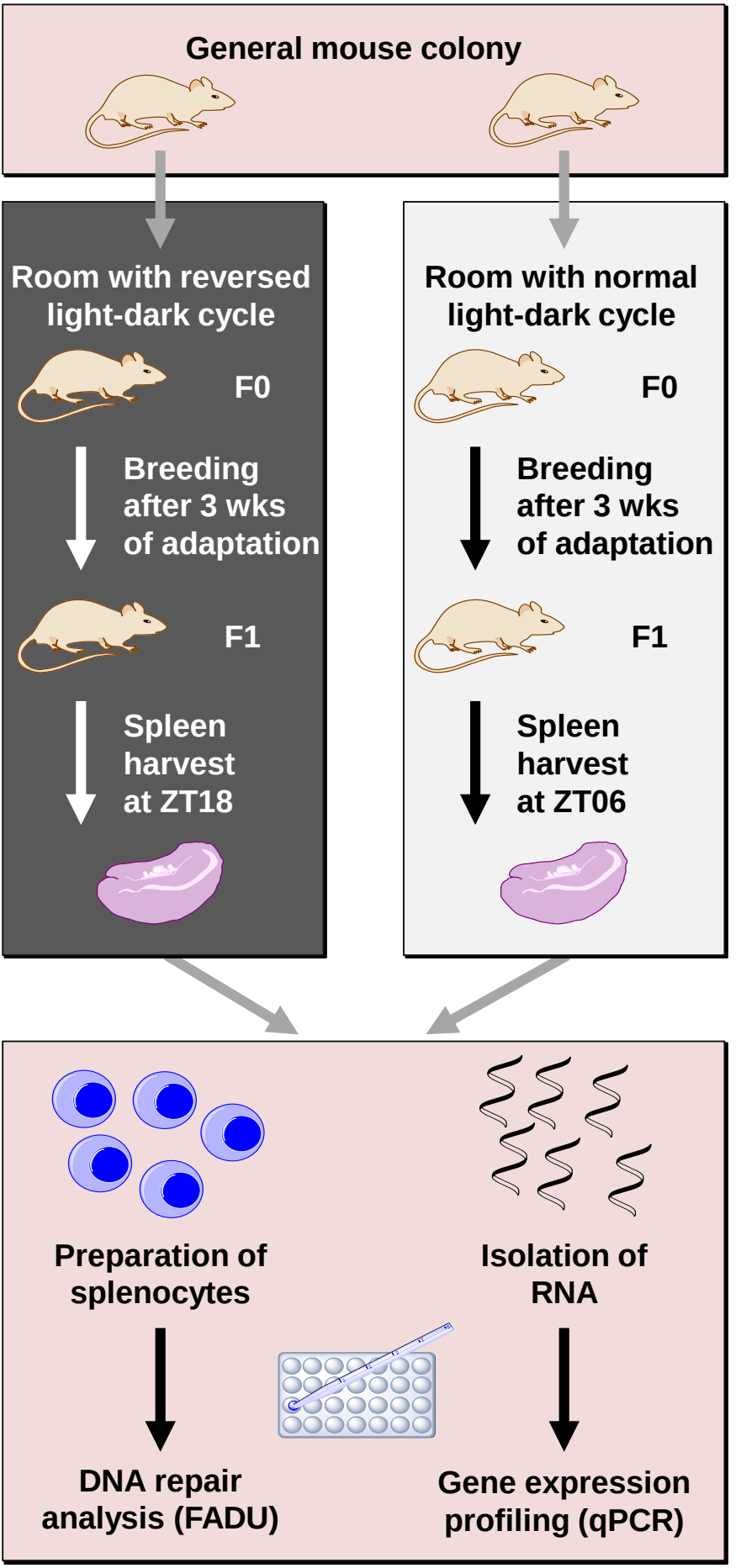
General mouse colony
Room with reversed light-dark cycle
F0
Breeding after 3 wks of adaptation
F1
Spleen harvest at ZT18
Room with normal light-dark cycle
F0
Breeding after 3 wks of adaptation
F1
Spleen harvest at ZT06
Preparation of splenocytes
Isolation of RNA
DNA repair analysis (FADU)
Gene expression profiling (qPCR)

Figure 2

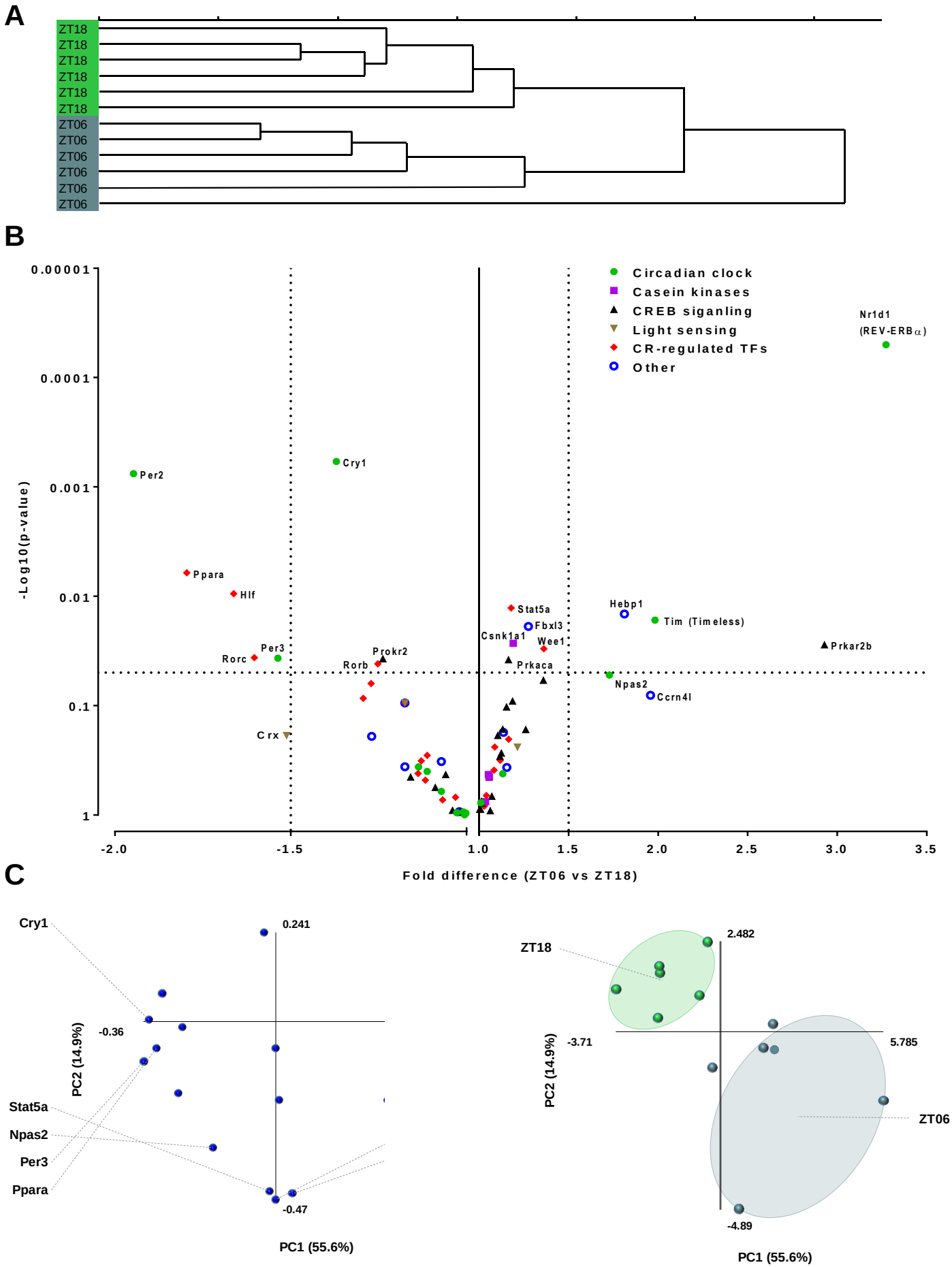
A
ZT18
ZT18
ZT18
ZT18
ZT18
ZT18
ZT06
ZT06
ZT06
ZT06
ZT06
ZT06
B
Circadian clock
Casein kinases
CREB siganling
Light sensing
CR-regulated TFs
Other
Nr1d1
(REV-ERBα)
Per2
Cry1
Ppara
Hlf
Per3
Rorc
Rorb
Prokr2
Crx
Stat5a
Fbxl3
Csnk1a1
Wee1
Prkaca
Hebp1
Tim (Timeless)
Prkar2b
Npas2
Ccrn4l
-Log10(p-value)
0.00001
0.0001
0.001
0.01
0.1
1
-2.0
-1.5
1.0
1.5
2.0
2.5
3.0
3.5
Fold difference (ZT06 vs ZT18)
C
Cry1
0.241
-0.36
PC2 (14.9%)
Stat5a
Npas2
Per3
Ppara
-0.47
PC1 (55.6%)
ZT18
2.482
-3.71
5.785
PC2 (14.9%)
ZT06
-4.89
PC1 (55.6%)

Figure 3

A

1 Preparation of cells
↓
2 DNA-damaging treatment
↓
3 DNA repair
↓
4 **Cell transfer**
⬇
5 **Lysis**
⬇
6 **DNA unwinding**
⬇
7 **Neutralization**
⬇
8 **SybrGreen® addition**
⬇
9 **Mixing**
↓
10 Fluorescence detection
↓
11 Data evaluation

B

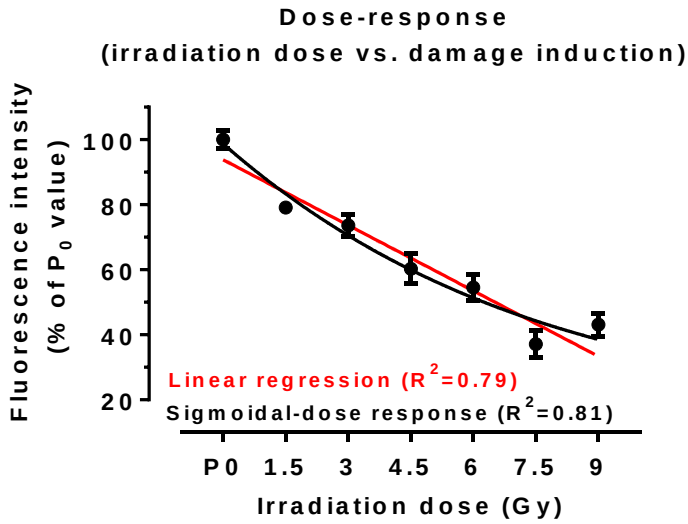

C

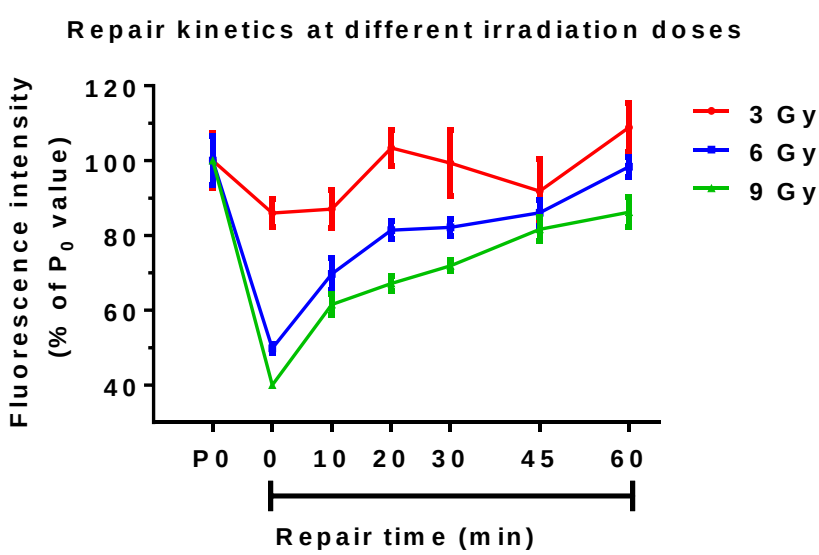

Figure 4

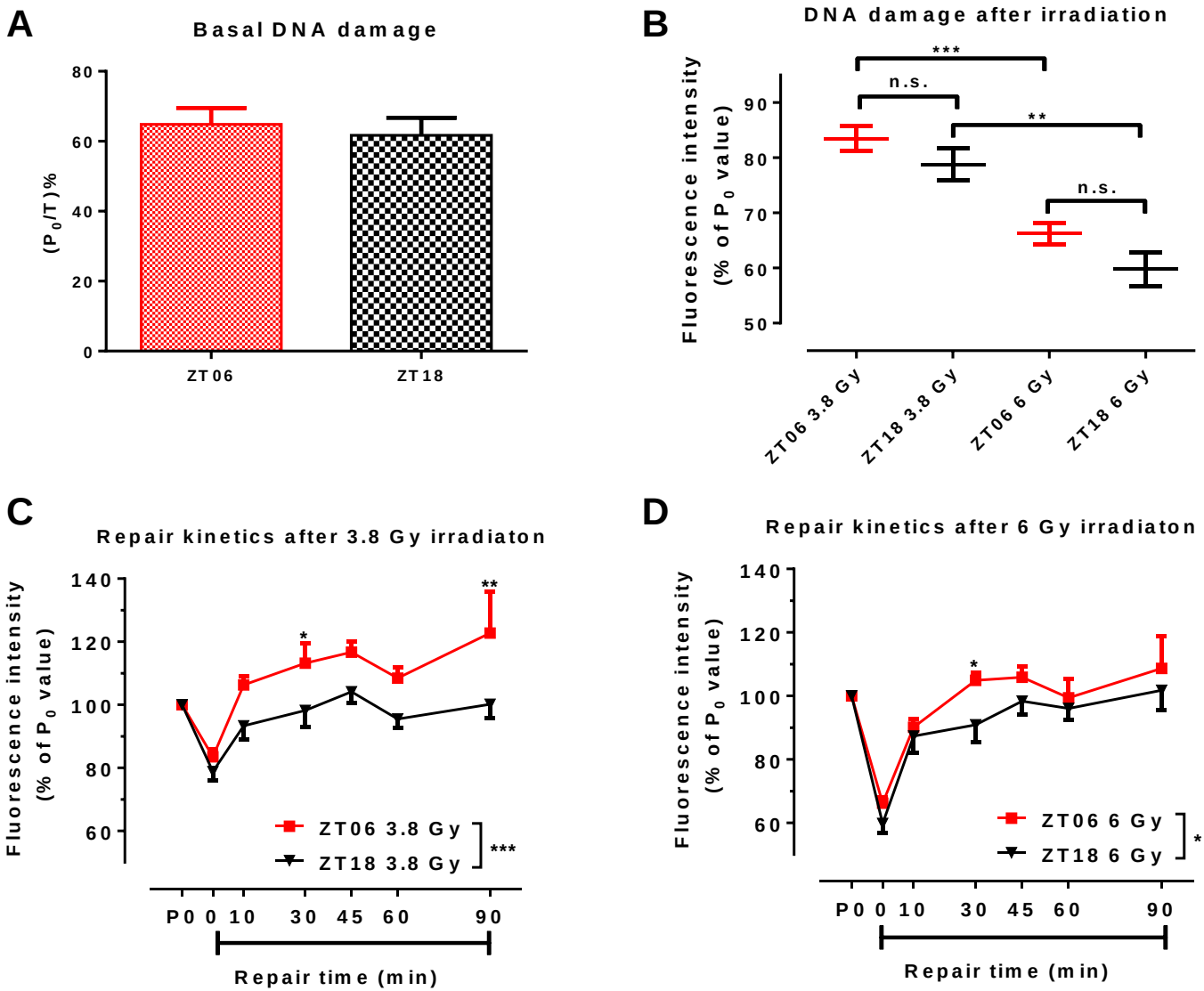
A
Basal DNA damage
(P0/T)%
80
60
40
20
0
ZT06
ZT18
B
DNA damage after irradiation
Fluorescence intensity
(% of P0 value)
90
80
70
60
50
***
n.s.
**
n.s.
ZT06 3.8 Gy
ZT18 3.8 Gy
ZT06 6 Gy
ZT18 6 Gy
C
Repair kinetics after 3.8 Gy irradiaton
Fluorescence intensity
(% of P0 value)
140
120
100
80
60
*
**
ZT06 3.8 Gy
ZT18 3.8 Gy
***
P0 0 10 30 45 60 90
Repair time (min)
D
Repair kinetics after 6 Gy irradiaton
Fluorescence intensity
(% of P0 value)
140
120
100
80
60
*
ZT06 6 Gy
ZT18 6 Gy
*
P0 0 10 30 45 60 90
Repair time (min)

Figure 5

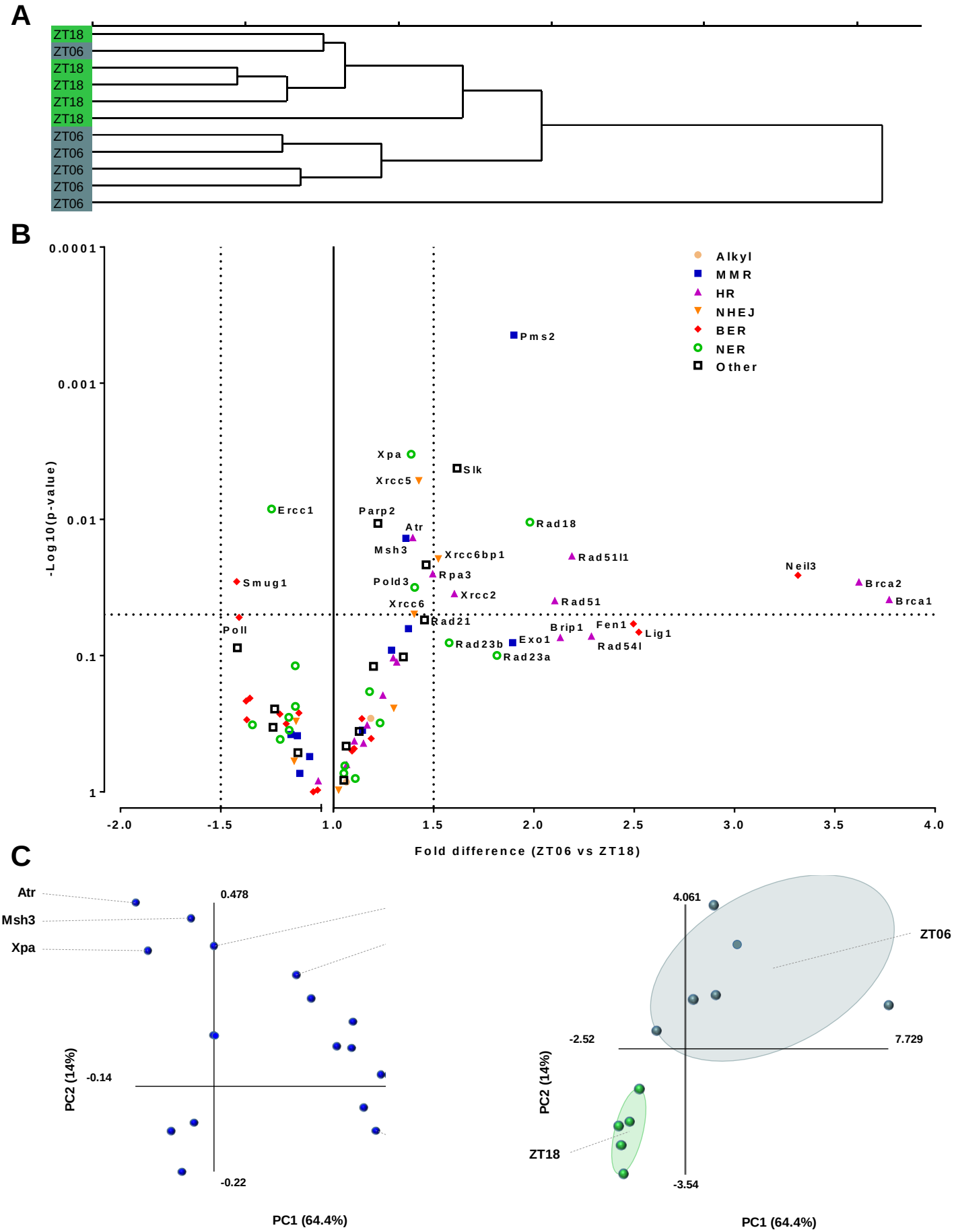
A
ZT18
ZT06
ZT18
ZT18
ZT18
ZT18
ZT06
ZT06
ZT06
ZT06
ZT06
B
Alkyl
MMR
HR
NHEJ
BER
NER
Other
Pms2
Xpa
Slk
Xrcc5
Ercc1
Parp2
Atr
Rad18
Msh3
Xrcc6bp1
Rad51l1
Neil3
Smug1
Pold3
Rpa3
Brca2
Xrcc2
Brca1
Xrcc6
Rad51
Rad21
Brip1
Fen1
Lig1
Poll
Rad23b
Exo1
Rad54l
Rad23a
-Log10(p-value)
0.0001
0.001
0.01
0.1
1
-2.0
-1.5
1.0
1.5
2.0
2.5
3.0
3.5
4.0
Fold difference (ZT06 vs ZT18)
C
Atr
Msh3
Xpa
0.478
-0.14
-0.22
PC2 (14%)
PC1 (64.4%)
4.061
ZT06
-2.52
7.729
ZT18
-3.54
PC2 (14%)
PC1 (64.4%)

Figure 6

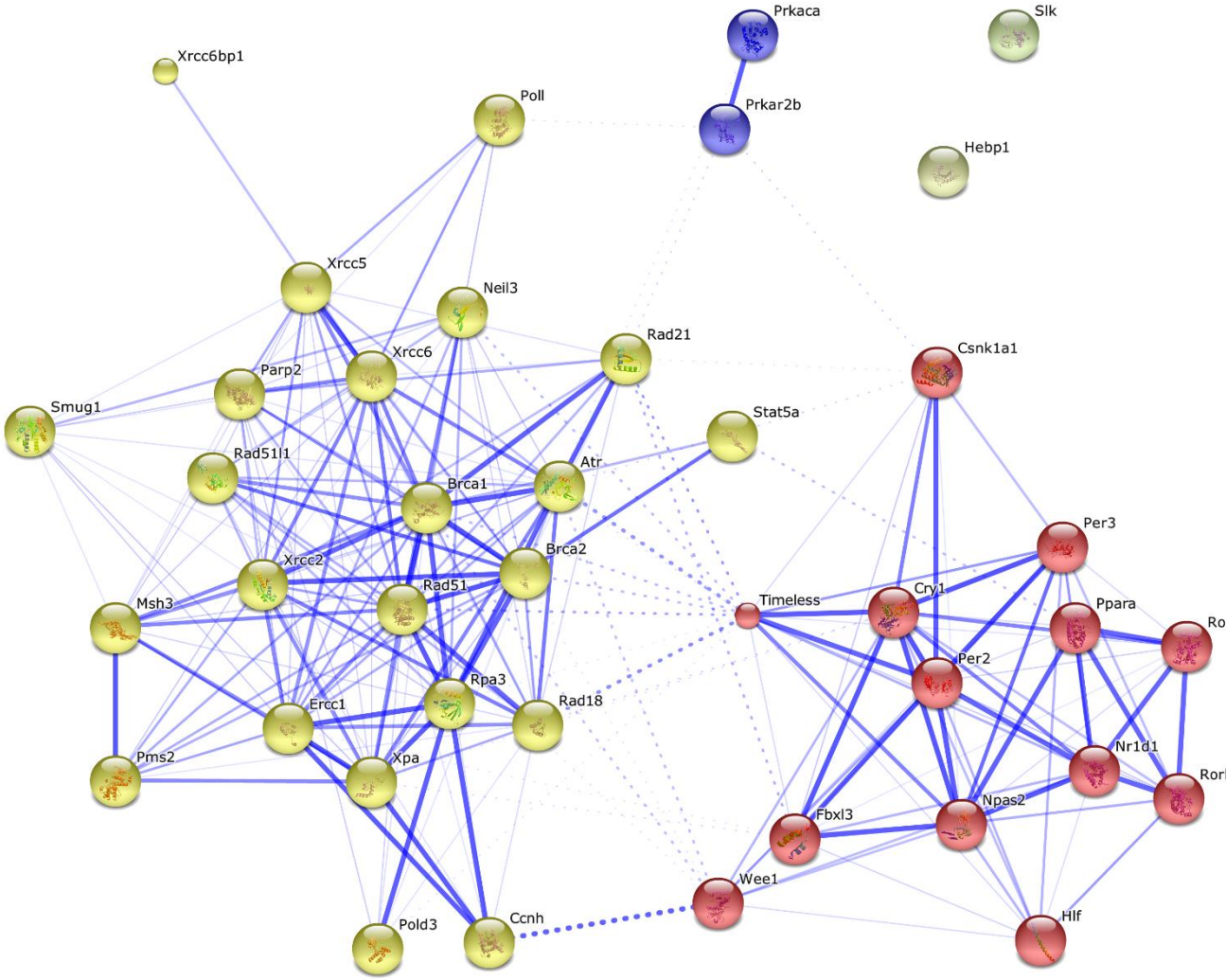
Prkaca
Slk
Xrcc6bp1
Poll
Prkar2b
Hebp1
Xrcc5
Neil3
Rad21
Csnk1a1
Xrcc6
Parp2
Smug1
Stat5a
Rad51l1
Atr
Brca1
Per3
Brca2
Xrcc2
Rad51
Cry1
Timeless
Ppara
Msh3
Rorc
Per2
Rpa3
Rad18
Ercc1
Nr1d1
Pms2
Xpa
Rorb
Npas2
Fbxl3
Wee1
Hlf
Pold3
Ccnh